

## Ionic Surface States from a Band-Edge Method

JULES D. LEVINE

*RCA Laboratories, Princeton, New Jersey*

AND

S. G. DAVISON

*Department of Applied Mathematics and Physics, University of Waterloo, Waterloo, Ontario, Canada*

(Received 29 May 1968)

The properties of surface states on ionic or partially ionic crystals such as NaCl, CdS, and GaAs have been computed using the method of linear combination of atomic orbitals (LCAO) in a novel way. The method consists of simulating an ionic crystal by assigning  $s$  and  $p$  orbitals on *alternate* sites in a one-dimensional crystal so that the resonance integral alternates in sign along a chain. This feature causes the band gap to lie at the center of the Brillouin zone, as required for these crystals. Also, the unperturbed reference energies are conveniently chosen to be the band-edge energies, rather than the separated-atom energies as in the more usual LCAO method. In an  $MX$  crystal,  $M$ -like states appear somewhat below the conduction band when the lattice is terminated at an  $M$  atom. Similarly,  $X$ -like states appear somewhat above the valence band when the lattice ends on an  $X$  atom. The results complement and support the previous Madelung and Mathieu theories for ionic surface states, and have the proper qualitative behavior to agree with experiment.

### I. INTRODUCTION

COMPARED to intrinsic surface states on Si and Ge crystals, the intrinsic surface states on ionic (or partially ionic) crystals such as NaCl, CdS, and GaAs have received comparatively little attention theoretically<sup>1-3</sup> or experimentally.<sup>4-10</sup> This situation is unusual in the respect that the Si and Ge surfaces are reconstructed<sup>11</sup> according to LEED (low-energy electron diffraction), whereas it seems that the ionic surfaces are not.<sup>12-14</sup> To be specific, the ionic surfaces of  $MX$  crystals such as (110) zinc blende, (11 $\bar{2}$ 0) wurtzite, and (100) NaCl have a lateral periodicity identical to the bulk and are natural cleavage surfaces. They have an equal number of  $M$  (metallic) and  $X$  (non-metallic) ions in the surface plane. Apparently, the lateral electrostatic forces stabilize these surfaces against reconstruction, even though the  $M$  and  $X$  ions generally have only a fractional charge. This is especially true for the III-V and II-VI compounds. Thus, there seems to be

more hope of comparing surface-state theory and experiment for these ionic surfaces than for the reconstructed Si or Ge surfaces.

Experimental evidence for ionic surface states has been accumulating gradually in the last few years.<sup>4-10</sup> The ionic surface states seem to have the following two properties. (1) They frequently appear in pairs: An  $M$ -like surface state that lies a few tenths of an eV below the conduction band edge, and an  $X$ -like surface state that lies a few tenths of an eV above the valence band. (2) The surface states frequently act as compensated traps in the more insulating crystals, and cause band bending in the more highly doped crystals. Then band bending is inversely related to the band gap.

The two theories that have successfully described these states are briefly reviewed below. The simplest is based on Madelung sums and classical electrostatics.<sup>1,2</sup> Essentially, the bulk ions are taken to be classical point ions with fractional charge. The surface ions are taken to be equivalent to the bulk ions, except that their Madelung energies are reduced because the Coulomb three-dimensional sums are over only *half*-space. Then since the bulk band gap is related to the bulk Madelung energy (in this classical model), there should be a reduced band gap at the surface and the  $M$  and  $X$  pairs of surface states should appear. The  $M$  (or  $X$ ) states arise when there is an  $M$  (or  $X$ ) ion in the surface plane. Surface-state energies in the few tenths of an eV range have been computed given the following: fractional ionic charge (e.g., 0.5 for CdS), first and second ionization potentials and electron affinities, internuclear spacing, crystal bulk type, and crystallographic direction, e.g., (110) zinc blende. Calculation shows that the smaller the band gap, the deeper the surface states, in agreement with experiment. There are two basic inadequacies of this model. The relationship of the model to the solution of a Schrödinger equation is not apparent, and the effects of band-broadening are not ex-

<sup>1</sup> J. D. Levine and P. Mark, Phys. Rev. **144**, 751 (1966).

<sup>2</sup> J. D. Levine, Proc. Am. Phys. Soc. **10**, 1093 (1965); and invited paper, Chicago American Physical Society Meeting, 1967 (unpublished).

<sup>3</sup> J. D. Levine, Phys. Rev. **171**, 701 (1968).

<sup>4</sup> P. Mark, RCA Rev. **26**, 461 (1965).

<sup>5</sup> P. Mark, J. Phys. Chem. Solids **26**, 959 (1965); **26**, 1767 (1965).

<sup>6</sup> G. A. Somorjai and J. E. Lester, J. Chem. Phys. **43**, 1450 (1965).

<sup>7</sup> R. K. Swank, Phys. Rev. **153**, 844 (1967).

<sup>8</sup> C. A. Mead, Solid-State Electron. **9**, 1023 (1966).

<sup>9</sup> W. Ruppel, in *II-VI Semiconducting Compounds: 1967 International Conference*, edited by D. G. Thomas (W. A. Benjamin, Inc., New York, 1967).

<sup>10</sup> H. R. Huff, S. Kawaji, and H. C. Gatos, J. Surface Sci. **10**, 232 (1968).

<sup>11</sup> J. J. Lander, J. Surface Sci. **1**, 125 (1964).

<sup>12</sup> I. Murklund and S. Anderson, J. Surface Sci. **5**, 197 (1966).

<sup>13</sup> L. P. Feinstein and D. P. Shoemaker, J. Surface Sci. **3**, 294 (1965).

<sup>14</sup> A. U. MacRae, J. Surface Sci. **4**, 247 (1966); also A. U. MacRae and G. W. Gobeli, in *Semiconductors and Semimetals*, edited by R. K. Willardson and A. C. Beer (Academic Press Inc., New York, 1966), Vol. 2, pp. 115-137.

plicitly included. These inadequacies will be resolved in the present paper.

The other theory developed for dealing with ionic surface states was designed to incorporate the exact solution of a Schrödinger equation.<sup>3</sup> The crystal potential is chosen to be one-dimensional and sinusoidal with variable amplitude. This amplitude is a measure of the "ionicity." The crystal is terminated at an arbitrary position in the last unit cell and with arbitrary step height. Inside the crystal, the Schrödinger equation reduces, in this case, to the Mathieu equation, whose properties are fortunately well known. Analysis shows that ionic states appear in the appropriate band gap and have the desired properties mentioned above. To be specific, a one-dimensional lattice terminated at an  $M$  ion (electropositive ion) has an  $M$ -like surface state that moves closer to the conduction band the greater the ionicity. Similarly, the lattice terminated at an  $X$  ion has an  $X$ -like surface state that moves closer to the valence band the greater the ionicity. These states appear in the second band gap which lies at the center  $\Gamma$  of the one-dimensional Brillouin zone.<sup>15</sup> This is the proper one-dimensional representation for ionic crystals as seen from two points of view. First, consider the simplest classical arguments. In a three-dimensional ionic crystal (such as NaCl), the  $s$  and  $p$  levels of Cl are filled, and these two are broadened to constitute the separate  $s$ - and  $p$ -valence bands of the crystal with the "first" band gap in between. Also, the  $s$ -like state of Na is empty and this constitutes the conduction band that lies above the Cl  $p$  band. Thus, the main or most important band gap between the top of the valence band and the bottom of the conduction band is the second. A much better argument can be obtained from observing the three-dimensional  $E(\mathbf{k})$  band structure constructed by others<sup>16</sup> for a variety of III-V and II-VI partially ionic crystals. In most cases, the band gap between the top of the valence band and the bottom of the conduction band lies at the center  $\Gamma$  of the three-dimensional Brillouin zone (BZ), whereas the first band gap (not of much interest for surface states) lies far below and at the edge of the BZ. The type of band gap at  $\Gamma$  is said to be "direct." It is simpler, in many respects, than the band gaps of Ge or Si, which are indirect.<sup>16</sup> Alkali halides have an indirect gap due to a valence-band maximum off  $\Gamma$ . There are still certain inadequacies of this one-dimensional Mathieu model. It cannot readily be extended to three dimensions, since the wave function must be matched at all points in the interface region, and the choice of a sinusoidal potential is somewhat restrictive unless other harmonics are added.

It is desirable, therefore, to compute ionic surface states by a third, independent method to further

strengthen and elucidate the theoretical basis of these states. Surely the more independent the methods which point to the same result, the greater the certainty of this result. The new method selected in this paper is called a band-edge LCAO (linear combination of atomic orbitals) method.

Since the conduction- and valence-band-edge energies are accurately known from a variety of theoretical and experimental studies on many  $MX$  crystals,<sup>16</sup> it seems wise to use these energies as firm starting points in the computation of surface states. In other words, no attempt will be made here to *predict* these band-edge energies; they are taken as inputs to the problem of ionic surface states. To be specific, the band-edge energies and wave functions are taken as exact eigenvalues and eigenfunctions of the Schrödinger equation, analogous to Ref. 3. In this manner, the location of the surface states within the band gap becomes more accurate and the comparison with experiment becomes more natural. The above proposed procedure differs from the more usual methods called LCAO or "tight-binding" methods in texts on solid-state theory,<sup>17</sup> or "MO-LCAO-Hückel" methods in texts on quantum chemistry.<sup>18</sup> In these more usual methods, the energies of the *separated atoms* (not the band-edge energies) are taken as the basic energies. For example, in some solid-state tests<sup>17</sup> the *separated-atom* energies and wave functions are taken as exact eigenvalues and eigenfunctions of the Schrödinger equation. In other solid-state texts,<sup>15</sup> the unperturbed energies  $E(\mathbf{k})$  are taken as the basis of LCAO perturbation theory. That is, the diagonal energies are functions of  $\mathbf{k}$ ; they are not the band-edge energy constants chosen here.

Accordingly the new procedure chosen in this paper will be called by a somewhat modified title—the "band-edge LCAO method"; its closest analog in the field of solid state is the  $\mathbf{k} \cdot \mathbf{p}$  method.<sup>19</sup> Also, its far-reaching appeal in the computation of surface states and comparison with experiment has not been recognized before, although certain of its aspects have already been derived by Davison and others<sup>20,21</sup> under the title "MO-LCAO method."

The ionic surface-state problem has an especially interesting feature. The  $s$  orbitals on the  $M$  sites and the  $p$  orbitals on the  $X$  sites create resonance integrals  $\beta$ , which *alternate in sign along* a chain. A mechanical analogy might be a chain with two different masses and two different spring constants alternating in sign along

<sup>17</sup> See, for example, J. M. Ziman, *Principles of the Theory of Solids* (Cambridge University Press, N. Y., 1964), p. 80; J. Callaway, *Energy Band Theory* (Academic Press Inc., New York, 1964), p. 102; H. Jones, *ibid.*, p. 216.

<sup>18</sup> See, for example, R. Daudel, R. Lefebvre, and C. Moser, *Quantum Chemistry* (Interscience Publishers, Inc., New York, 1959), p. 52.

<sup>19</sup> M. Cardona, *J. Phys. Chem. Solids* **24**, 1543 (1963); also M. Cardona and F. H. Pollack, *Phys. Rev.* **142**, 530 (1966).

<sup>20</sup> S. G. Davison and J. Koutecký, *Proc. Phys. Soc. (London)* **89**, 237 (1966).

<sup>21</sup> A. T. Amos and S. G. Davison, *Physica* **30**, 905 (1964).

<sup>15</sup> H. Jones, *Theory of Brillouin Zones and Electronic States in Crystals* (North-Holland Publishing Co., Amsterdam, 1962).

<sup>16</sup> See, for example, M. L. Cohen and T. K. Bergstresser, *Phys. Rev.* **141**, 789 (1966).

the chain. But this mechanical system would be inherently unstable, so that there is no *simple* mechanical analogy. By contrast, if one would have *s* orbitals on the even (odd) sites and, say, other *s* orbitals on the odd (even) sites, all  $\beta$ 's would be the *same* sign along a chain. Then the mechanical analogy would be the usual sort of chain with two different masses and a positive force constant. The band gap would occur at the *edge* rather than the *center* of the BZ. This is the case treated previously by Davison and others<sup>20-22</sup> using two-band LCAO theory, and it is also the case treated in diatomic-crystal phonon-band theory.<sup>23,24</sup> It is *not* the case applicable to ionic surface states.

It will be convenient and instructive to formulate the band-edge LCAO model in one dimension by following closely Levine's Mathieu and Madelung problems as guides. That is, a deliberate attempt will be made to construct parallels in formalism and notation between these various approaches. This will demonstrate that one can view ionic surface states in a variety of representations, which are readily interchangeable. Also, the results will be rearranged at the end to be consistent with Davison's notation.<sup>20</sup> This will demonstrate the new features of the present problem within the more traditional LCAO context.

A following paper will extend the method of this problem to three dimensions. Some new features then appear such as light- and heavy-valence bands and spin-orbit coupling. Detailed comparison with experiment will be carried out at the end of that paper.

Very recently, the ionic-like surface states of InSb surfaces have been interpreted using dangling-bond concepts and combinations of Tamm- and Shockley-state concepts,<sup>10</sup> but no attempt was made to assign energy levels using the concepts. These "dangling-bond" concepts complement, in a qualitative way, the Madelung, Mathieu, and band-edge LCAO methods which seem more explicit and better suited to computation of energy levels. It should be noted, in passing, that the (111), (111), and (100) surfaces of InSb are probably reconstructed so that the dangling bonds are partly saturated; this has not been taken into account in the analysis of the authors.<sup>10</sup>

II. BULK

Consider a one-dimensional representation of a semi-infinite ionic crystal of the type *MX* as shown schematically in Fig. 1. The *M* (metallic) atoms are located at odd numbered sites  $n=1, 3, 5, \dots$ ; their valence atomic orbitals  $\phi_M$  have *s*- or *d*-like symmetry. By contrast, the *X* (non-metallic) atoms are located at even-

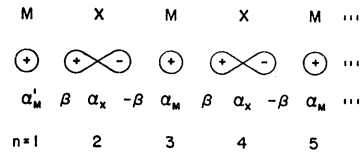


FIG. 1. Essential aspects of a one-dimensional ionic semi-infinite chain showing the *M* and *X* atoms, their orbital-wavefunction symmetry types, Coulomb and resonance integrals, and location with respect to the end of the chain ( $n=1$ ).

numbered sites  $n=2, 4, 6, \dots$ ; their valence atomic orbitals  $\phi_X$  have *p*-like symmetry. To be specific, upon reflection about the atom centers of Fig. 1, the respective orbitals become  $\phi_M \rightarrow \phi_M$  and  $\phi_X \rightarrow -\phi_X$ . The alternation in atomic-orbital symmetry type along the chain is the main characteristic of ionic or partially ionic crystals. In general, the ionicity is fractional, so that the components of the crystal can be called atoms or ions equivalently.

Let the conduction band-edge energy be called  $\alpha_M$  and its wave function be called  $\psi_M^0$ . These eigenvalues and eigenfunctions satisfy, by definition,  $H\psi_M^0 = \alpha_M\psi_M^0$ . From three-dimensional band-structure studies<sup>16</sup> of most ionic or partially ionic crystals  $\psi_M^0$  has symmetry  $\Gamma_1$ , so that upon reflection  $\psi_M^0 \rightarrow \psi_M^0$ . Also,  $\alpha_M$  lies at the center of the BZ as shown in Fig. 2.

Similarly, let the valence band-edge energy be called  $\alpha_X$  and its wave function be called  $\psi_X^0$ . These satisfy  $H\psi_X^0 = \alpha_X\psi_X^0$ . From three-dimensional band-structure studies of cubic and zinc-blende crystals (no spin-orbit coupling)  $\psi_X^0$  has symmetry<sup>16</sup>  $\Gamma_{15}$ , which is equivalent to the triply degenerate  $p_x, p_y, p_z$  wave functions.<sup>15</sup> Since the one-dimensional representation of Fig. 1 is to be used,  $\psi_X^0$  is chosen to be *p<sub>z</sub>*-like so that upon reflection  $\psi_X^0 \rightarrow -\psi_X^0$ . A following paper will show that the additional *p<sub>x</sub>*- and *p<sub>y</sub>*-like valence bands form two heavy-hole bands, but that few new types of surface states appear, so that *p<sub>x</sub>* and *p<sub>y</sub>* can be safely ignored

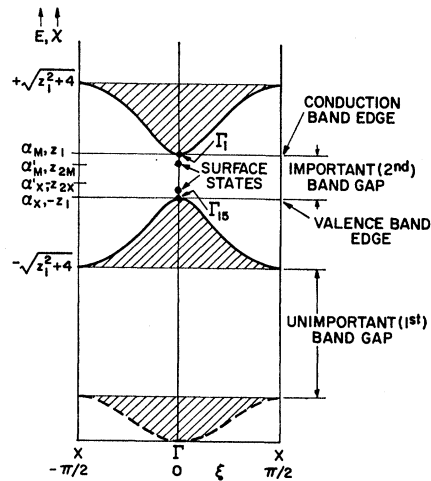


FIG. 2. One-dimensional representation of the band structure of an ionic or partially ionic crystal with a cubic lattice.

<sup>22</sup> T. A. Hoffman, *Acta Phys. Hungaricae* **1**, 175 (1951) (in English).

<sup>23</sup> F. Seitz, *The Modern Theory of Solids* (McGraw-Hill Book Co., New York, 1940), pp. 277, 121.

<sup>24</sup> A. A. Maraududin, E. W. Montroll, and G. H. Weiss, *Theory of Lattice Dynamics in the Harmonic Approximation* (Academic Press Inc., New York, 1963).

for the present. Note that  $\alpha_X$  also lies at the center of the BZ in Fig. 2 and  $\alpha_M > \alpha_X$ .

It is logical to expand  $\psi_M^0$  and  $\psi_X^0$  in terms of atomic orbitals on  $M$  and  $X$  sites, respectively, with *similar* symmetry properties as follows:

$$\psi_M^0 = \sum_{n=1,3,5}^{\infty} \phi_M(z-n), \quad (1a)$$

$$\psi_X^0 = \sum_{n=2,4,6}^{\infty} \phi_X(z-n). \quad (1b)$$

In this form  $\psi_M^0$  and  $\psi_X^0$  have identical symmetry properties to the Mathieu functions<sup>3</sup>  $ce_2(z,q)$  and  $se_2(z,q)$ , respectively. These border the second band gap as desired in the ionic-crystal problem.<sup>3</sup>

It is desirable to create Bloch waves  $\psi_M$  and  $\psi_X$ , which closely resemble the band-edge functions  $\psi_M^0$  and  $\psi_X^0$ . This is done by using the basic LCAO relations

$$\psi_M = \sum_{n=1,3,5}^{\infty} a_n \phi_M(z-n), \quad (2a)$$

$$\psi_X = \sum_{n=2,4,6}^{\infty} a_n \phi_X(z-n), \quad (2b)$$

$$a_n = \exp(in\theta), \quad (3)$$

$$\theta = \xi + i\mu, \quad \xi \text{ and } \mu \text{ real.} \quad (4)$$

Note that, for  $\theta=0$ ,  $\psi_M = \psi_M^0$  and  $\psi_X = \psi_X^0$  as required. The Bloch condition is satisfied in the sense that  $\psi_M(z+2) = \exp(2i\theta)\psi_M(z)$ .

An adequate representation of surface states within the band gap, or bulk states near the conduction or valence band edges, can be made by forming a hybrid as follows:

$$\psi = \psi_M + R\psi_X, \quad (5)$$

where  $R$  is a hybridizing parameter, analogous to  $\lambda$  of Ref. 3 and  $K$  of Ref. 20. Of course, for very thin bandwidths compared to the band gap, other band-edge hybrids must be added on to Eq. (5) to yield a more reasonable representation of the surface or bulk states. Fortunately, this situation is not serious for most crystals.<sup>16</sup> The consequences of including other hybrids are relatively minor, as shown in Ref. 3, except for the very lowest band edge in Fig. 2, which becomes a metallic (or virtual) surface state.

The crystal energy  $E$  is obtained from using the Schrödinger equation

$$(H-E)\psi = 0 \quad (6)$$

and the usual LCAO integrals of the form<sup>20,21</sup>

$$H_{nn'} = \int \phi_n^*(z-n) H \phi_{n'}(z-n') dz, \quad (7)$$

where  $n$  or  $n'$  can be odd or even. Specifically,

$$\begin{aligned} H_{nn} &= \alpha_M & n \text{ odd} \\ &= \alpha_X & n \text{ even.} \end{aligned} \quad (8)$$

These are commonly called "Coulomb" integrals, even though there is a kinetic-energy contribution in  $H$ . Also, the nearest-neighbor integrals are

$$\begin{aligned} H_{n, n+1} &= -H_{n, n-1} = \beta & n \text{ odd} \\ &= -\beta & n \text{ even.} \end{aligned} \quad (9)$$

These are commonly called nearest-neighbor resonance integrals. All other integrals are ignored here. Note that  $\beta$  alternates in sign along a chain; this can also be seen from inspection of Fig. 1. Also, note that the surface  $M$  atom ( $n=1$ ) has a different Coulomb integral

$$H_{11} = \alpha_M'. \quad (10)$$

(On the other hand, suppose that the lattice started as  $n=2, 3, 4, \dots, \infty$ . Then, the end atom would be  $X$ , and one would have  $H_{22} = \alpha_X'$ .) It will be shown below that the *sign* of  $\beta$  does not affect the presence or absence of surface states; the results are dependent only on the *alternation in sign* of  $\beta$  from one site to the next. To solve for  $E$ , multiply Eq. (6) by  $\phi_M^*(z-n)$  and integrate. Then do the same with  $\phi_X^*(z-n)$ . These operations combined with Eqs. (2), (5), and (7)–(9) yield the recursion relations

$$\beta a_{n+1} - \beta a_{n-1} + R(\alpha_M - E)a_n = 0 \quad n \text{ odd}, \quad (11)$$

$$(\alpha_X - E)a_n - R\beta a_{n+1} + R\beta a_{n-1} = 0 \quad n \text{ even}. \quad (12)$$

Note that because of Eq. (5), all  $a_l$  with  $l$  odd must have  $R$  as a coefficient. Equations (11) and (12) are only valid for  $n > 1$ .

Combining Eqs. (3), (11), and (12), one has the matrix for the "bulk" states

$$\begin{bmatrix} \alpha_M - E & 2i\beta \sin\theta \\ -2i\beta \sin\theta & \alpha_X - E \end{bmatrix} \begin{bmatrix} R \\ 1 \end{bmatrix} = 0. \quad (13)$$

The solution of the secular equation is

$$E = \frac{1}{2} \{ \alpha_M + \alpha_X \pm [(\alpha_M - \alpha_X)^2 + 16\beta^2 \sin^2\theta]^{1/2} \}. \quad (14)$$

Note that  $\beta$  gives the curvature of the band edges at  $\theta=0$ ; it can therefore be roughly determined by using effective-mass measurements. In other words, the values  $\alpha_M$ ,  $\alpha_X$ ,  $\beta$  can be determined from experiment and the integrals in Eqs. (7)–(9) need not be explicitly evaluated.

Using the definitions

$$\begin{aligned} \bar{\alpha} &= \frac{1}{2}(\alpha_M + \alpha_X), \\ \chi &= (E - \bar{\alpha})/\beta, \\ z_1 &= (\alpha_M - \alpha_X)/2\beta, \end{aligned} \quad (15)$$

Eq. (14) becomes

$$\chi = \pm (z_1^2 + 4 \sin^2\theta)^{1/2}. \quad (16)$$

This is similar to Eq. (2.2) of Ref. 20 except that, because of the alternation in sign of  $\beta$ ,  $\cos^2\theta$  is here replaced by  $\sin^2\theta$ . The bulk energies can be obtained easily by setting  $\mu=0$ , i.e.,  $\theta=\xi$ . Then Eqs. (14) and (16) yield the desired bulk-band spectrum, drawn, for example, taking  $z_1=0.5$ , in Fig. 2. The main (valence-to-conduction) band gap occurs at  $\xi=0$ , not at  $\xi=\frac{1}{2}\pi$ , which is the case in Refs. 20 and 21.

Next, consider the possibility of a surface state such that  $\theta=\xi+i\mu$  in Eq. (16). For the wave function to be exponentially damped into the crystal, one must have  $\mu>0$ . For the energy to be real it is necessary that  $\text{Im}(\sin^2\theta)=0$  or

$$\sin 2\xi \sinh 2\mu = 0. \quad (17)$$

One solution of this is  $\mu=0$ , but this is the bulk spectrum described above. The *ionic surface states* are defined from the combination

$$\begin{aligned} \xi &= 0, \quad \mu > 0, \\ a_n &= \exp(-n\mu). \end{aligned} \quad (18)$$

Their energies, obtained from Eqs. (16) and (18), are

$$\chi = \pm (z_1^2 - 4 \sinh^2 \mu)^{1/2}, \quad (19)$$

and they lie inside the band gap as desired for these states. These states are sometimes called inner-surface states.<sup>20</sup> Outer states are obtained from the combination

$$\begin{aligned} \xi &= \pm \frac{1}{2}\pi, \quad \mu > 0, \\ a_n &= (-1)^{1/2n} \exp(-n\mu). \end{aligned} \quad (20)$$

The coefficients  $a_n$  and  $a_{n+2}$  alternate in sign along a chain and the energies

$$\chi = \pm (z_1^2 + 4 \cosh^2 \mu)^{1/2} \quad (21)$$

lie outside the allowed bands. But these outer states<sup>20</sup> are not consistent with the assumptions inherent in Eq. (5), so they will be neglected here. Moreover, it is the ionic or inner states, not the outer states, that are experimentally detected. Finally, consider the only other combination which also satisfies Eq. (17), viz.,

$$\begin{aligned} \xi &= \pi, \quad \mu > 0, \\ a_n &= (-1)^n \exp(-n\mu). \end{aligned} \quad (22)$$

This combination yields the same energies as Eq. (19), but  $a_n$  for  $n$  odd (even) has a negative (positive) sign. Recalling that  $\psi_M$  and  $\psi_X$  are LCAO functions located on odd and even sites, respectively, one sees that in Eq. (5) the change  $\xi=0 \rightarrow \xi=\pi$  is identical to the change  $R \rightarrow -R$ . It will be shown later that the properties of ionic surface states are not affected by this *consistent* transformation  $R \rightarrow -R$ . Therefore, the choices  $\xi=0$  and  $\xi=\pi$  are *equivalent*.<sup>25</sup> From a band-structure point of view, the energies and wave functions at the center of a one-dimensional Brillouin zone of a diatomic

<sup>25</sup> This equivalence was not pointed out by Davison and Koutecký (see Ref. 20).

crystal ( $M$ - $M$  spacing is two units) are specified by *either*  $\xi=0$  or  $\xi=\pi$ . That is, the states at  $\xi=0$  and  $\xi=\pi$  are not distinguishable. This is a basic result of the translational symmetry of the one-dimensional crystal. Similarly, the states at  $\xi=+\frac{1}{2}\pi$ ,  $-\frac{1}{2}\pi$  are not distinguishable. For simplicity and clarity, therefore, Eq. (22) will be ignored since it yields no new results. [Note added in proof. These complications disappear if the  $M$ - $M$  or  $X$ - $X$  distances are taken as unity, instead of the  $M$ - $X$  distance as assumed above. Then  $\theta \rightarrow \frac{1}{2}\theta$  and the equivalent states are  $0$ ,  $2\pi$ , and  $\pi$ ,  $-\pi$ . Also the Bloch condition takes the more familiar form  $\Psi_M(z+1) = \exp(i\theta)\Psi_M(z)$ .]

To find  $R$  for the ionic surface state ( $\alpha_X < E < \alpha_M$  and  $\theta=i\mu$ ) Eqs. (13) and (18) are used to obtain

$$R = (2\beta \sinh \mu)(\alpha_M - E)^{-1}. \quad (23)$$

Since  $\mu > 0$  and  $\alpha_M > E$ , it follows that

$$R/\beta > 0. \quad (24)$$

This is a necessary condition for a surface state; it is independent of the sign of  $\beta$ . (The case of  $R/\beta < 0$  corresponds physically to  $\mu < 0$ , which is an exponentially *increasing* wave function and must be rejected.) It is possible to rearrange Eqs. (13) and (23) to yield some useful relationships:

$$\frac{R}{\beta} = \frac{1}{|\beta|} \left( \frac{E - \alpha_X}{\alpha_M - E} \right)^{1/2}, \quad (25a)$$

$$E = (\alpha_X + R^2 \alpha_M) / (1 + R^2), \quad (25b)$$

$$4\beta^2 \sinh^2 \mu = (\alpha_M - E)(E - \alpha_X), \quad (25c)$$

which have direct analogs with Ref. 3. Note that when  $R \rightarrow 0$ ,  $E \rightarrow \alpha_X$  and  $\mu=0$ ; when  $R \rightarrow 1$ ,  $E \rightarrow \bar{\alpha}$  and  $\mu$  is a maximum; when  $R \rightarrow \infty$ ,  $E \rightarrow \alpha_M$  and  $\mu=0$ . For  $R$  imaginary either  $E > \alpha_M$  or  $E < \alpha_X$  and  $\mu$  becomes imaginary so that a Bloch wave is formed in the conduction or valence bands.

### III. SURFACE

The  $\mu$  values for the ionic surface states, which have so far remained unspecified, will now be determined from the surface matching conditions.

#### $M$ Atom

For a termination on an  $M$  atom ( $n=1$ ) as shown in Fig. 1, Eq. (11) yields

$$R(\alpha_M' - E)a_1 + \beta a_2 = 0. \quad (26)$$

Combine this with Eq. (18) to yield

$$E = \alpha_M' + \beta e^{-\mu} / R. \quad (27)$$

Since from Eq. (11),  $R/\beta > 0$ , one must have

$$\alpha_M' < E < \alpha_M. \quad (28)$$

This is the existence condition for an *M*-like surface state. Thus,  $\alpha_M'$  must lie below the  $\alpha_M$  level as shown in Fig. 2. This result is independent of the sign of  $\beta$  as assumed earlier. The "bulk" equations (11) and (12) can be written in the forms

$$E = \alpha_M - \beta(e^\mu - e^{-\mu})/R, \tag{29}$$

$$E = \alpha_X + \beta(e^\mu - e^{-\mu})R. \tag{30}$$

These equations indicate that the Schrödinger equation is satisfied within the "bulk." They are *equivalent* in the sense that they both yield the *same*  $E$ , provided the same value of  $R$  be used.

Eliminate  $E$  from Eqs. (27) and (29) to get

$$\beta e^\mu / R = \alpha_M - \alpha_M'. \tag{31}$$

Next, eliminate  $\beta/R$  from Eqs. (31) and (27) to yield

$$E = \alpha_M' + (\alpha_M - \alpha_M') \exp(-2\mu). \tag{32}$$

This demonstrates that Eq. (28) is correct, since  $\mu > 0$ . Equivalent but much more awkward expressions for *M*-like states can be obtained by eliminating  $E$  from Eqs. (27) and (30), instead of Eqs. (27) and (28). Using the definitions

$$z_{2M} = (\alpha_M' - \bar{\alpha})/\beta, \tag{33a}$$

$$L = \exp(-2\mu), \tag{33b}$$

Eqs. (32), (28), and (19) become

$$\chi = z_{2M} + (z_1 - z_{2M})L, \tag{34a}$$

$$\chi = z_1 - (z_1 - z_{2M})(1 - L), \tag{34b}$$

$$z_{2M} < \chi < z_1, \tag{34c}$$

$$\chi = \pm [z_1^2 - (1 - L)^2 L^{-1}]^{1/2}. \tag{34d}$$

Note that, since  $0 < \mu < \infty$ , the allowed range of  $L$  is  $0 < L < 1$ . Also, note from Eq. (33) that  $L$  is unchanged if  $\mu$  is replaced by  $\mu \rightarrow i\pi + \mu$ . This again shows that all  $\chi$  of interest are independent of the choice  $\xi = 0$  or  $\xi = \pi$  as presumed earlier.

Eliminating  $\chi$  from Eqs. (34b) and (34d) yields

$$p_M L^2 + q_M L - 1 = 0, \tag{35}$$

where

$$p_M = (z_1 - z_{2M})^2, \tag{36a}$$

$$q_M = 1 + z_1^2 - z_{2M}^2, \tag{36b}$$

$$r_M = p_M q_M^{-2}. \tag{36c}$$

The root of Eq. (35) for  $0 < L < 1$  is

$$2p_M L = -q_M + (q_M^2 + 4p_M)^{1/2} \tag{37a}$$

or

$$L = \frac{1}{q_M} \left( \frac{-1 + (1 + 4r_M)^{1/2}}{2r_M} \right). \tag{37b}$$

As can be seen from Eqs. (36a) and (36c),  $r_M$  is always positive. It can be shown that the term in the brackets in Eq. (37b) is always less than unity and positive for

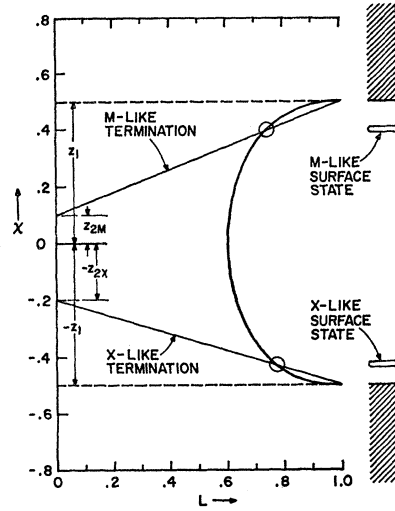


Fig. 3. Graphical solution of the surface-state problem. The *M*- and *X*-like surface states appear as the intersections of the surface and bulk relations.

all  $r_M$ . The same is true for the coefficient  $q_M^{-1}$ , since Eq. (34c) applies. Therefore,  $0 < L < 1$  as required in Eq. (33b) and there is an allowed solution of Eqs. (37a) and (37b) for all  $z_1$  and  $z_{2M}$ , provided that  $z_1 > z_{2M}$ . This is true even if  $z_{2M}$  is negative. Substitution of Eq. (37b) in Eq. (34a) yields  $\chi$  as an explicit function of  $z_1, z_{2M}$ .

The mathematics can be considered in another way by using a graphical method as shown in Fig. 3. Here  $\chi$  is plotted versus  $L$  in the physically meaningful range  $0 < L < 1$ . The *C*-shaped curve with extrema  $\pm z_1$  is a plot of the bulk relation Eq. (34d). To be specific,  $z_1$  is chosen for the figure to be  $z_1 = 0.5$ . The straight line sloping upwards from  $z_{2M}$  to  $z_1$  is the surface relation Eq. (34b), which applies to a termination on an *M* atom. The intersection of the curve and the line gives the *M*-like surface state as shown in the figure. There is also a trivial intersection at  $\chi = z_1$ , but this occurs at  $L = 1$  or  $\mu = 0$ , so this is just the allowed (*M*-like) conduction band-edge state. From this graph one can see that there will always be a nontrivial intersection (surface state) provided that  $z_1 > z_{2M}$ . If  $z_{2M}$  is negative enough, the negative sign of Eq. (34d) may be the appropriate solution, in which case  $\chi < 0$ . In any case, there is at most one (surface-state) solution for any fixed value of  $z_{2M}$ , even though the "bulk" relation Eq. (34d) seems to be double-valued.

The  $L$  parameter has a simple physical significance as seen from writing Eq. (34b) in the form

$$L = \frac{(z_1 - z_{2M}) - (z_1 - \chi)}{z_1 - z_{2M}} = \frac{KE}{PE}. \tag{38}$$

Referred to the conduction band edge, the *M*-like surface state has a "trap" energy equal to  $z_1 - \chi$  and a "potential energy" (PE) equal to  $z_1 - z_{2M}$  in dimensionless notation. The difference between these energies is

the “kinetic energy” (KE) of the electron in the surface-state trap. Thus,  $L$  is simply the ratio of KE to PE in the surface-state trap. For example, in Fig. 2,  $L=0.8$  for the  $M$ -like surface states. Note from Eq. (33b) that  $0 < L < 1$ , so  $KE < PE$ . For fairly shallow surface states,  $r_M$  is small, so that the square root can be expanded to give

$$L \sim q_M^{-1} = (1 + z_1^2 - z_2^2)^{-1}. \quad (39)$$

This shows that the ratio KE/PE, is smaller for crystals with wider band gaps  $\sim 2z_1$  and deeper surface-state potential energies  $\sim z_1 - z_{2M}$ .

The problem can be summed up as follows. From Eq. (37b),  $L$  is obtained; from Eq. (33b),  $\mu$  is obtained; from Eq. (32),  $E$  is obtained; and from Eq. (31),  $R$  is obtained. Thus, in principle, the  $M$ -like surface-state problem is solved.

#### X Atom

For a termination on an  $X$  atom (instead of the  $M$  atom shown in Fig. 1), the equations analogous to Eqs. (26)–(28) are

$$(\alpha_X' - E)a_2 - \beta R a_3 = 0, \quad (40a)$$

$$E = \alpha_X' - \beta R \exp(-\mu), \quad (40b)$$

$$\alpha_X < E < \alpha_X'. \quad (40c)$$

This is the existence condition for an  $X$ -like surface state. Thus,  $\alpha_X'$  must lie above the  $\alpha_X$  level as shown in Fig. 2 and the result is also independent of  $\beta$ .

The equations analogous to Eqs. (31)–(34) are

$$\beta R \exp(\mu) = \alpha_X' - \alpha_X, \quad (41a)$$

$$E = \alpha_X' - (\alpha_X' - \alpha_X) \exp(-2\mu), \quad (41b)$$

$$z_{2X} = -(\alpha_X' - \bar{\alpha})/\beta, \quad (41c)$$

$$\chi = -z_{2X} - (z_1 - z_{2X})L, \quad (41d)$$

$$-z_1 < \chi < -z_{2X}. \quad (41e)$$

Equation (34d) is unaltered for  $X$ -like surface states. Equivalent but much more awkward expressions would be obtained if, for  $X$ -like states, Eq. (29) were used instead of Eq. (30). Also, Eqs. (35)–(37) apply here except that  $z_{2M}$  is everywhere replaced by  $z_{2X}$ .

The  $X$ -like state can also be formed graphically. In Fig. 3, Eq. (41d) is drawn as a straight line sloping downwards; its intersection with the bulk solution, Eq. (34d), yields the  $X$ -like surface state as shown. There seems to be a strong formal similarity between the properties of  $M$ - and  $X$ -like surface states.

Before completing this analysis, consider again the consequences of selecting Eq. (22) as a condition for surface states instead of Eq. (18). The switch from  $\theta = i\mu$  to  $\theta = \pi + i\mu$  is equivalent to setting  $R \rightarrow -R$  in Eq. (5) and in *all* subsequent equations containing  $R$ , even Eq. (24). But the existence conditions for surface states [Eqs. (28) and (40c)] and their energies  $E$  have

been shown to be independent of  $R$ , provided that the *same*  $R$  is used throughout. In fact, the energies are dependent only on  $L = \exp(2i\theta)$ , so  $L$  is unchanged by switching from  $\theta = i\mu$  to  $\theta = \pi + i\mu$ . This demonstrates that Eqs. (22) and (18) yield equivalent surface states, so that one is justified in ignoring Eq. (22). Stated another way, the ionic surface states arise at the center  $\Gamma$  of the BZ in Fig. 2, which is characterized by  $\xi = 0$  or  $\xi = \pi$  interchangeably.

#### IV. DISCUSSION AND CONCLUSIONS

The results of this band-edge LCAO method closely complement and support those of the Mathieu<sup>3</sup> and Madelung<sup>1,2</sup> methods. The Mathieu analogy can best be seen by comparing the matrix, Eq. (13), with the comparable matrix of the Mathieu problem (for small band gap) rewritten here to yield consistent notation:

$$\begin{bmatrix} a_m - E & -2\pi^{-1}K_{mm}\mu \\ 2\pi^{-1}K_{mm}\mu & b_m - E \end{bmatrix} \begin{bmatrix} \lambda \\ 1 \end{bmatrix} = 0. \quad (42)$$

Here,  $m$  is the band-gap index, and for ionic surface states  $m=2$ .  $a_2 = \alpha_M$  and  $b_2 = \alpha_X$ , so that the diagonal elements are the identical band-edge energies in both the LCAO and Mathieu problems.

The off-diagonal terms in the Mathieu problem contain the  $\mathbf{k} \cdot \mathbf{p}$ -like integral in dimensionless form, since

$$K_{mm} \equiv \int_0^{2\pi} ce_m(z, q) \left( \frac{d}{dz} \right) se_m(z, q) dz. \quad (43)$$

This integral couples the  $ce_m(z, q)$  and  $se_m(z, q)$  functions, which are the band-edge wave functions of the top and bottom, respectively, of the  $m$ th band gap. By comparison, the off-diagonal term in Eq. (13) of the LCAO problem contains an integral of the resonance type with strength  $\beta$  as shown in Eqs. (7) and (9). It also couples the band edges, but in a somewhat different way. In any case, the off-diagonal term  $\beta$  gives the curvature to the band edges, as shown in Fig. 2, and can thus be determined from effective-mass experiments.

In the Mathieu problem, the  $\lambda$  parameter hybridizes the  $se_m(z, q)$  and  $ce_m(z, q)$  functions, while in the LCAO problem the  $R$  parameter hybridizes the  $\psi_M$  and  $\psi_X$  functions.

There are also similarities with regard to the surface-matching equations. Both  $\lambda$  and  $R$  are uniquely determined by these equations, and the existence conditions for surface states are essentially  $\lambda > 0$  and  $R > 0$ . This similarity holds even though the Mathieu problem requires equating the values and slopes of  $\psi$  at the surface  $z_0$ , while the LCAO problem simply removes atoms to the left of the surface ( $a_0 = 0$ ,  $a_{-1} = 0$ ,  $a_{-2} = 0$ , etc.).

It is also illuminating to relate this band-edge LCAO method to the Madelung problem. There the band-edge energies are simply taken as  $\alpha_M$  and  $\alpha_X$  and the surface-state energies are simply taken as  $\alpha_M'$  and  $\alpha_X'$ . This

simplicity is a consequence of the lack of a quantum-mechanical foundation in the Madelung problem. In other words, in the classical Madelung problem the off-diagonal terms containing  $\mu$  are absent. These terms containing  $\mu$ , as shown in Eqs. (32) and (41b), add kinetic energy and cause the  $M$ - and  $X$ -like surface-state energies to approach somewhat closer to their respective band edges. Also, the classical Madelung problem contains no bulk bandwidth; this is a consequence of the absence of off-diagonal terms containing  $\beta$ .

The main advantage of the Madelung problem is that it is strongly based in chemistry and electrostatics. Undoubtedly, the Coulomb-energy differences  $\alpha_M - \alpha_{M'}$  and  $\alpha_{X'} - \alpha_X$  can be computed by the Madelung method much more reliably than by using the LCAO integrals. This follows because the details of the local potential and wave functions in the surface and bulk needed for Eqs. (8) and (10) in the LCAO method are not known. To be specific, the three-dimensional Madelung model<sup>1,2</sup> of an ionic solid strongly indicates that  $\alpha_M > \alpha_{M'}$  and  $\alpha_{X'} > \alpha_X$ , as shown in Fig. 2. This follows because the surface Madelung constant is less than the bulk, and the Madelung energy acts with equal strength, but in opposite directions, on the  $M$  and  $X$  ions.<sup>1,2</sup> Also, the surface and bulk Coulomb energies are fairly realistically computed in the Madelung method by taking the usual sort of Coulomb sum over *all* ions in the respective half and full spaces. In this manner one can *augment* the usefulness and accuracy of the band-edge LCAO method by evaluating  $\alpha_M - \alpha_{M'}$  and  $\alpha_{X'} - \alpha_X$  from the three-dimensional Madelung method.

This completes the discussion of ionic surface states using the one-dimensional band-edge LCAO method. It has been successfully integrated with the Mathieu

and Madelung methods, and displays the main features experimentally observed briefly in the Introduction. A more complete and quantitative comparison with experiment will be carried out in a following paper, where this band-edge LCAO method is extended to three dimensions. [*Note added in proof.* P. Mark has kindly pointed out to one of us (J. D. L.) that the above band-edge method has other useful features. These become apparent when the separated-atom energies of  $M$  and  $X$  species are explicitly included. Then the atomic  $M$  level is raised by the Coulomb term  $\int \phi_M^* \Delta V_M \phi_M dv$  and the atomic  $X$  level is lowered by the term  $\int \phi_X^* \Delta V_X \phi_X dv$ . Here  $\Delta V_M$  and  $\Delta V_X$  are the antisymmetric parts of the crystal potential in the  $M$  and  $X$  cells, respectively. The band-edge states then correspond to  $\alpha_M$  and  $\alpha_X$ , respectively. The classical limit<sup>1,2</sup> follows by using  $\delta$  functions for  $\phi_M$  and  $\phi_X$  and by using the Madelung potential for  $\Delta V$ .

Recently, it has been proved [J. D. L. (to be published)] that the above surface-state problem and the problem considered in Refs. 20 and 21 should have, in fact, *identical* energies, although the wave functions have a phase shift. A number of errors in Refs. 20 and 21 have thus been uncovered. Details will be given in a review article "Quantum theory of surface states" by the authors (S. G. D. and J. D. L.), in *Solid State Physics*, edited by F. Seitz and D. Turnbull (Academic Press, Inc., New York, to be published).]

#### ACKNOWLEDGMENTS

One of us (S. G. D.) wishes to acknowledge the support of the National Research Council of Canada, the Ontario Department of University Affairs, and the University of Waterloo Research Committee.